

Climatology, seasonality and trends of oceanic coherent eddies

Josué Martínez-Moreno¹, Andrew McC. Hogg¹, and Matthew England²

¹Research School of Earth Science and ARC Center of Excellence for Climate Extremes, Australian National University, Canberra, Australia

²Climate Change Research Centre (CCRC), UNSW Australia, Sydney NSW, Australia

Key Points:

- Kinetic energy climatology reveals a surprising heterogeneity in the global ocean.
- Transient kinetic energy show significant increasing trends over large areas of the Southern Ocean and the Northern Hemisphere.
- Regional kinetic energy climatology strongly depends to the region dominant oceanic process.

Abstract

Ocean eddies influence regional and global climate through mixing and transport of heat and properties. One of the most recognizable and ubiquitous feature of oceanic eddies are vortices with spatial scales of tens to hundreds of kilometers, frequently referred as “mesoscale eddies” or “coherent eddies”. Coherent eddies are known to transport properties across the ocean and to locally affect near-surface wind, cloud properties and rainfall patterns. Although coherent eddies are ubiquitous, yet their climatology, seasonality and long-term temporal evolution remains poorly understood. Thus, we examine the kinetic energy contained by coherent eddies and we present the annual, interannual, and long-term changes of automatically identified coherent eddies from satellite observations and a state of the art numerical simulation from 1993 to 2018. Satellite observations show that around 40% of the kinetic energy contained by ocean eddies corresponds to coherent eddies. Additionally, a strong hemispherical seasonal cycle is observed, on top of a 3–6 months lag between the wind forcing and the response of the coherent eddy field. Furthermore, the seasonality of the number of coherent eddies and their amplitude reveals that the number of coherent eddies responds faster to the forcing (~ 3 months), while the coherent eddy amplitude is lagged by ~ 6 months. There are regions that show a pronounced influence of coherent eddies, notably, the East Indian Ocean, the East Tropical Pacific Ocean, and the South Atlantic Ocean. In these locations, a strong seasonal cycle and interannual variability can be observed in both satellite and numerical models. Although, there is agreement between these products on the seasonality of the number of eddies, the seasonality of the coherent eddy amplitude between these products show some inconsistencies. Long-term trends of the coherent eddy amplitude from satellite observations and the state of the art model show significant increases in the eddy amplitude of $\sim 3\text{cm}$ per decade in large portions of the ocean, while the number of coherent eddies remains constant. Our analysis highlight the relative importance of the coherent eddy field in the ocean kinetic energy budget, imply a strong response of the eddy number and eddy amplitude to the surface wind at different time-scales, and showcases for the first time seasonality, and multidecadal trends of the coherent eddy properties.

Plain summary

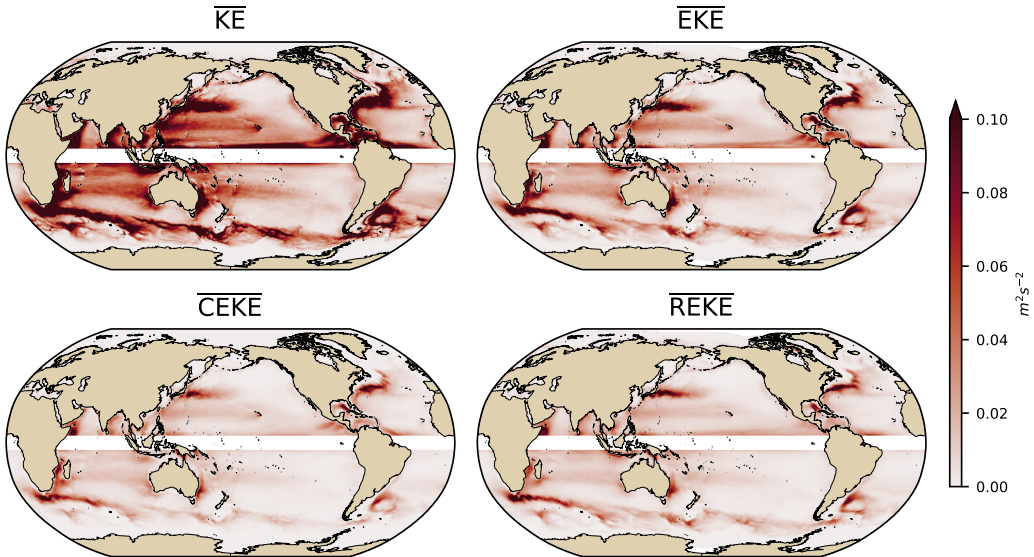


Figure 1. Replace REKE with nCEKE Climatology of surface kinetic energy (\overline{KE}), surface eddy kinetic energy (\overline{EKE}), surface coherent eddy kinetic energy (\overline{CEKE}), and surface non-coherent eddy kinetic energy (\overline{nCEKE}) between 1993-2018.

- Ratios of KE!! - Coherent signature + seasonality and non-coherent signature (not key point)
- Identify regions dominated by coherent eddies

1 Introduction

Ocean currents are highly anisotropic and include coherent vortices and meandering jets. While coherent vortices (recirculating currents) are approximated as ellipses with axes smaller than the Rossby radius of deformation (R_D), meandering jets are narrow but elongated currents. The anisotropic nature of these features translates in ...

2 Methods

3 Results

3.1 Coherent Eddy Energetics

3.1.1 Global

- Figure 1 shows regions with high values of Kinetic Energy at the Western Boundary Currents, ACC, and ocean gyres.

- $\overline{\text{EKE}}$ Explains 70% of $\overline{\text{KE}}$, while $\overline{\text{CEKE}}$ is 40% of $\overline{\text{EKE}}$ and $\overline{\text{nCEKE}}$ is 60% of $\overline{\text{EKE}}$
- Maps show that $\overline{\text{KE}}$, $\overline{\text{EKE}}$, $\overline{\text{CEKE}}$, and $\overline{\text{nCEKE}}$ are dominated by the western boundary currents, the Antarctic Circumpolar Current (ACC).

Note that nCEKE has a large amount of energy at high latitudes, this could be a consequence of the satellites not resolving the mesoscale coherent eddies.

3.1.2 Seasonality

3.2 Coherent Eddy Statistics

3.2.1 Global

Make sure to mention dipoles in the boundary currents.

-

Although these algorithms use different identification criteria, the spatial pattern of the number of eddies is consistent between them.

The maximum positive coherent eddy amplitude is commonly located polewards of the major boundary currents, while the maximum negative coherent eddy amplitude is found equatorwards. This is consistent to how coherent eddies are shed from these boundary currents.

3.2.2 Seasonality

3.3 Regional

```
Number 295.85546403962104 Pos amp 0.12094501820533601 Neg amp -0.1385068018754378
Chelton Number 236.7010877964295 Chelton Pos amp 7.779538694987785 Chelton Neg
amp -10.075637745571715 ACCESS Number 315.24697840283096 ACCESS Pos amp 0.0875635001289238
ACCESS Neg amp -0.08147261526708122
```

```
Number 207.37973697877084 Pos amp 0.08901200544912018 Neg amp -0.08816744392087235
Chelton Number 155.8983449906741 Chelton Pos amp 5.461227370020861 Chelton Neg
amp -5.348246201100335 ACCESS Number 243.4991508883295 ACCESS Pos amp 0.05249108358772637
ACCESS Neg amp -0.04136883487182314
```

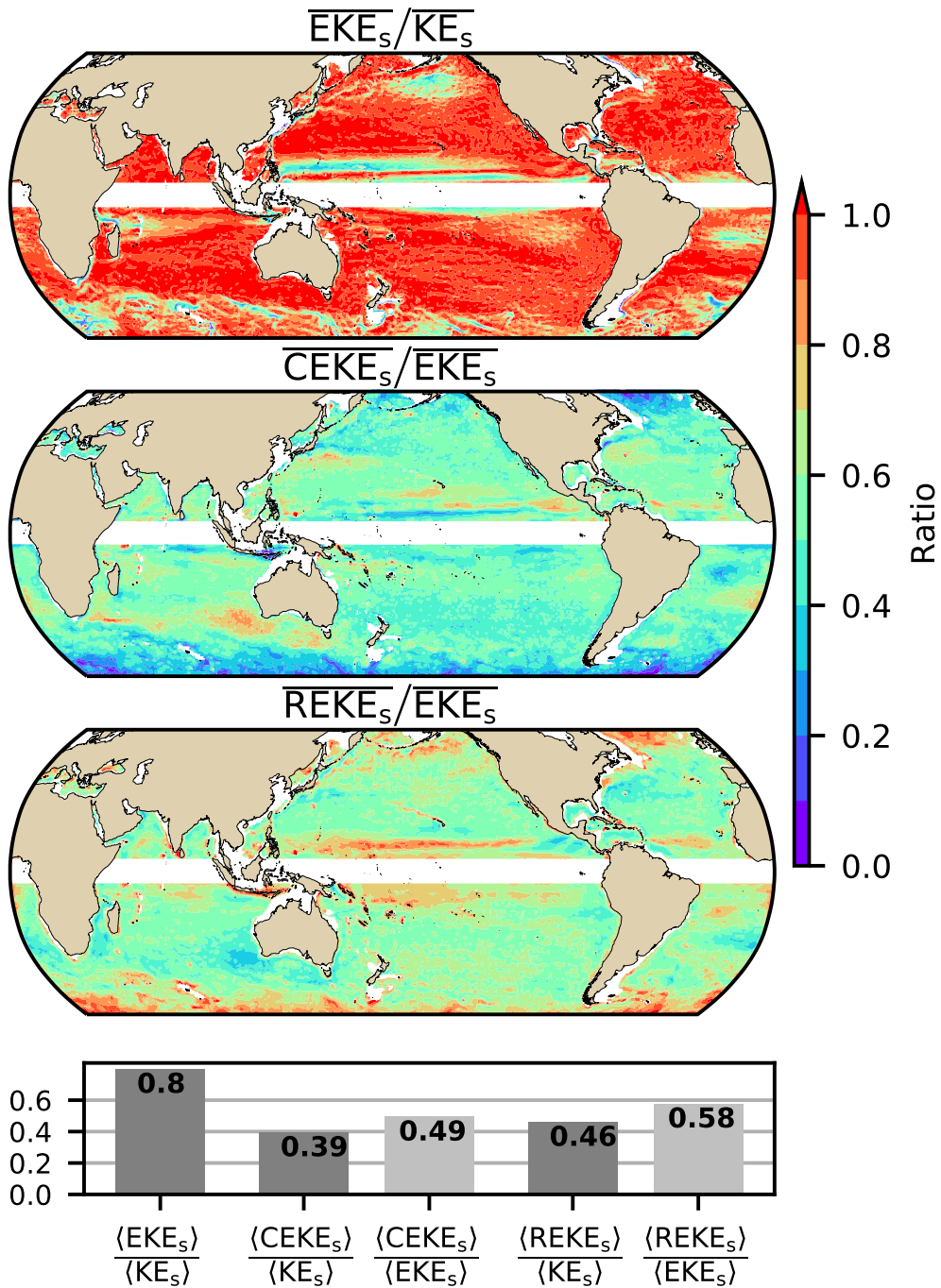


Figure 2. Replace REKE with nCEKE Ratios of the kinetic energy components. a) Map of the proportion of mean eddy kinetic energy (EKE) versus mean kinetic energy (\overline{KE}); b) Map of the proportion of mean coherent eddy kinetic energy (\overline{CEKE}) versus mean eddy kinetic energy (\overline{EKE}); c) Map of the proportion of mean non-coherent eddy kinetic energy (\overline{nCEKE}) versus mean eddy kinetic energy (\overline{EKE}); d) Global ratios of mean eddy kinetic energy ($\langle \overline{EKE} \rangle$), mean coherent eddy kinetic energy ($\langle \overline{CEKE} \rangle$) and mean non coherent eddy kinetic energy ($\langle \overline{nCEKE} \rangle$) versus the global mean kinetic energy ($\langle \overline{KE} \rangle$) and global mean eddy kinetic energy ($\langle \overline{EKE} \rangle$).

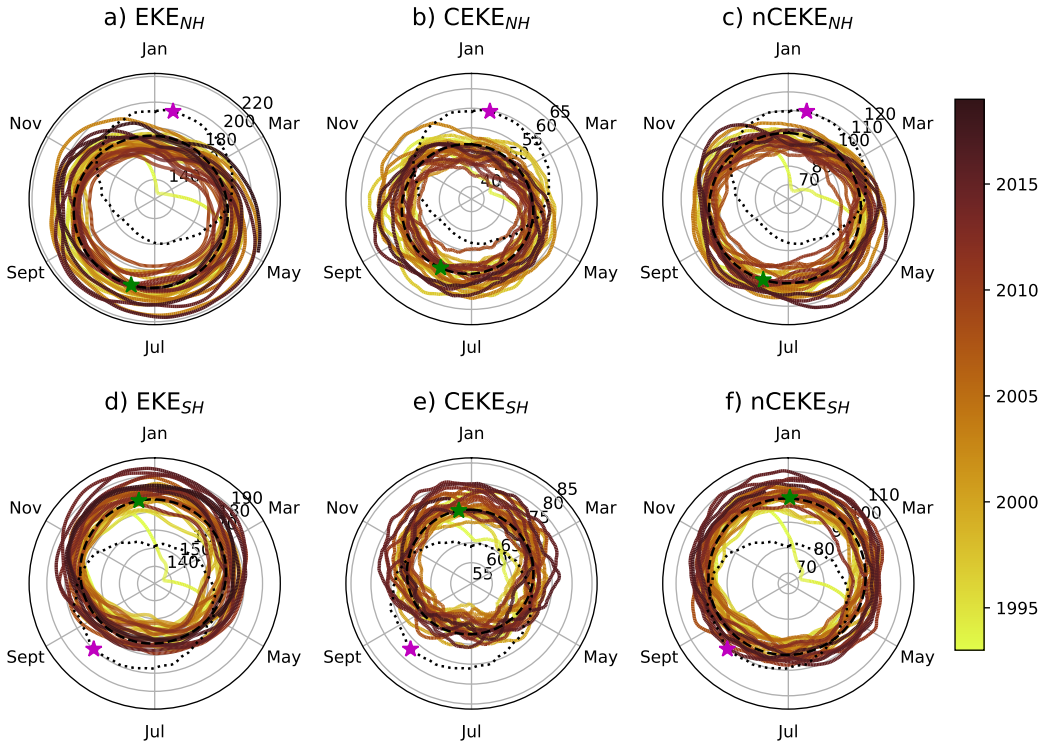


Figure 3. Hemispherical seasonality of eddy kinetic energy (EKE), coherent eddy kinetic energy (CEKE), and non-coherent eddy kinetic energy (nCEKE). Panels a,b and c show the northern hemisphere seasonal cycle, while panels d,e, and f correspond to the southern hemisphere. Dashed lines correspond to the seasonal climatology of the fields and dotted lines show the climatology of the wind magnitude. The green and magenta stars show the maximum of the seasonal cycle for the kinetic energy components and the wind magnitude, respectively. The line colors show the year.

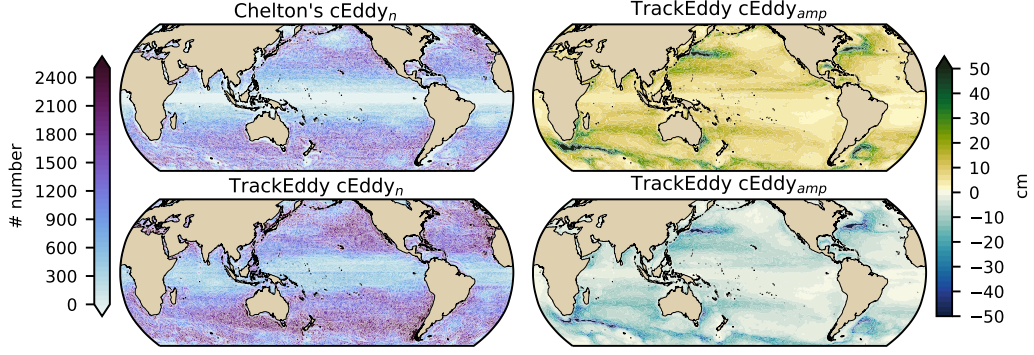


Figure 4. Climatology of the coherent eddy statistics. a) Climatology of the number of coherent eddies ($cEddy_n$) identified by Chelton et al. (2007); b) Climatology of the warm core coherent eddy amplitude ($cEddy_{amp}$). c) Climatology of the number of coherent eddies ($cEddy_n$) identified by Martínez-Moreno et al. (2019); d) Climatology of the cold core coherent eddy amplitude ($cEddy_{amp}$).

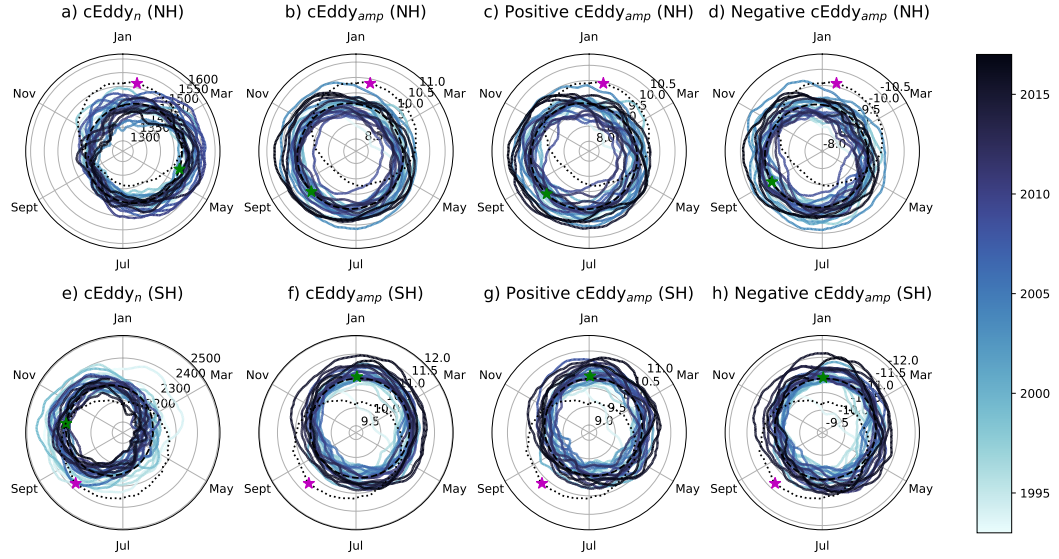


Figure 5. Hemispherical seasonality of the coherent eddy statistics; a,e) seasonal cycle of the number of coherent eddies ($cEddy_n$); b,f) seasonal cycle of the mean coherent eddy amplitude ($cEddy_{amp}$); c,g) seasonal cycle of the warm core coherent eddies amplitude ($wcEddy_{amp}$); d,h) seasonal cycle of the cold core coherent eddies amplitude ($ccEddy_{amp}$). Panels a,b and c show the northern hemisphere seasonal cycle, while panels d,e, and f correspond to the southern hemisphere. Dashed lines correspond to the seasonal climatology of the fields and dotted lines show the climatology of the wind magnitude. The green and magenta stars show the maximum of the seasonal cycle for the kinetic energy components and the wind magnitude, respectively. The line colors show the year.

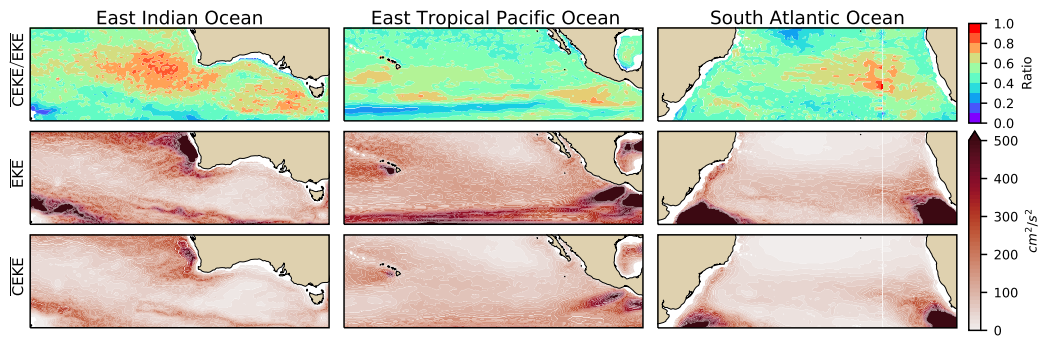


Figure 6. Climatology of regional statistics of the eddy field and coherent eddy field for the East Indian Ocean, East Tropical Pacific Ocean and South Atlantic Ocean. a-c Ratio of coherent eddy kinetic energy CEKE versus eddy kinetic energy EKE; d-f mean eddy kinetic energy (\overline{EKE}); g-i mean coherent eddy kinetic energy (\overline{CEKE}).

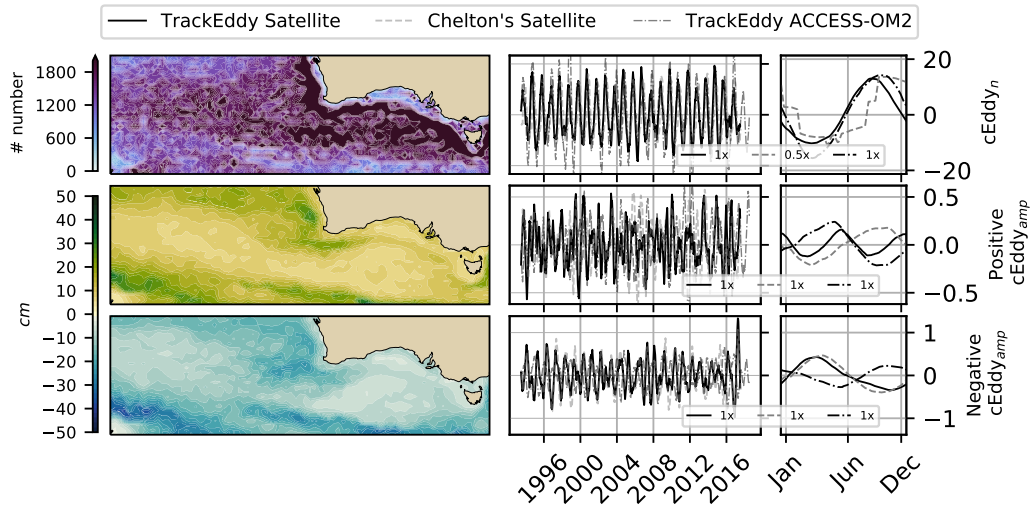


Figure 7. Climatology of regional statistics of the eddy field and coherent eddy field for the East Indian Ocean, East Tropical Pacific Ocean and South Atlantic Ocean. a-c Zoom to ratio of CEKE and EKE; d-f mean eddy kinetic energy (\overline{EKE}); g-i mean coherent eddy kinetic energy (\overline{CEKE}); j-k count of identified coherent eddies between 1993-2019; and l-n mean coherent eddy amplitude between 1993-2019.

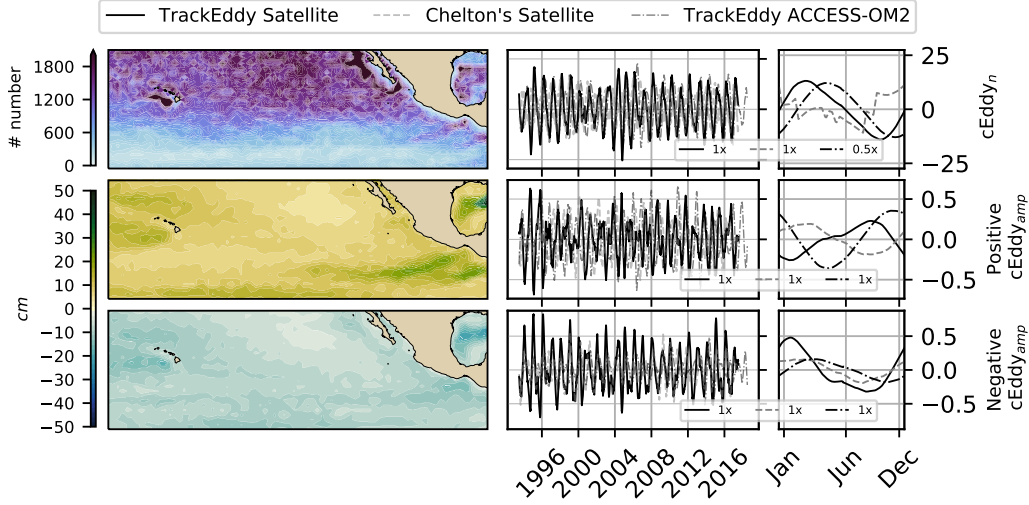


Figure 8. Climatology of regional statistics of the eddy field and coherent eddy field for the East Indian Ocean, East Tropical Pacific Ocean and South Atlantic Ocean. a-c Zoom to ratio of CEKE and EKE; d-f mean eddy kinetic energy (\overline{EKE}); g-i mean coherent eddy kinetic energy (\overline{CEKE}); j-k count of identified coherent eddies between 1993-2019; and l-n mean coherent eddy amplitude between 1993-2019.

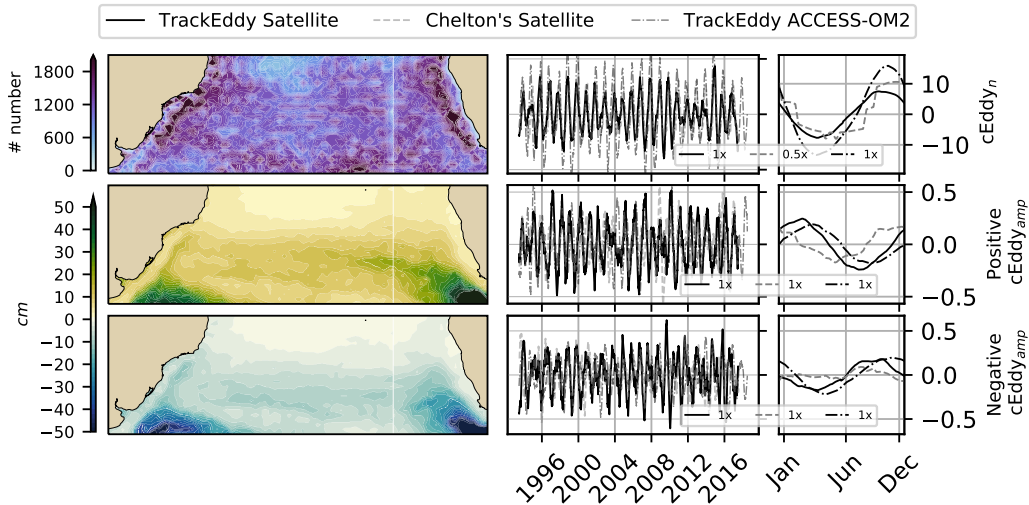


Figure 9. Climatology of regional statistics of the eddy field and coherent eddy field for the East Indian Ocean, East Tropical Pacific Ocean and South Atlantic Ocean. a-c Zoom to ratio of CEKE and EKE; d-f mean eddy kinetic energy (\overline{EKE}); g-i mean coherent eddy kinetic energy (\overline{CEKE}); j-k count of identified coherent eddies between 1993-2019; and l-n mean coherent eddy amplitude between 1993-2019.

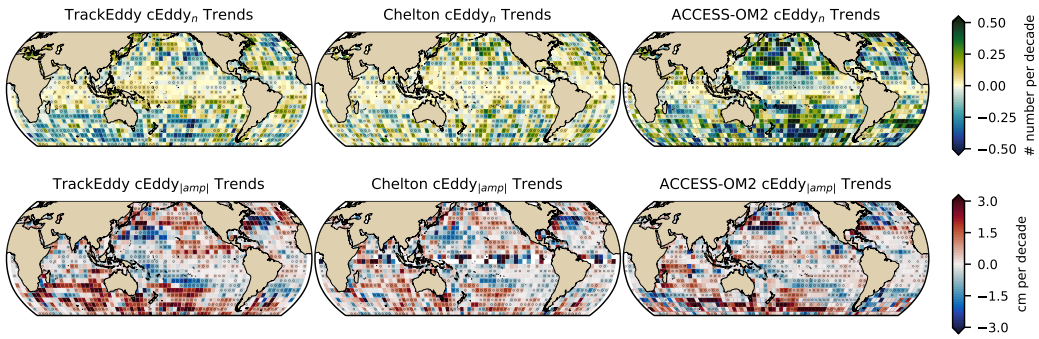


Figure 10. **Crop colorbar** Trends of coherent eddy statistics. a,b and c Trends of the number of identified coherent eddies from satellite observations identified using TrackEddy, satellite observations identified using Chelton's, and state of the art numerical simulation identified using TrackEddy. d,e and f Trends of the sum of the absolute value of identified coherent eddies amplitude from satellite observations identified using TrackEddy, satellite observations identified using Chelton's, and state of the art numerical simulation identified using TrackEddy. Gray stippling shows regions that are statistically significant above the 95% confidence level.

```

Number 228.35682569539446 Pos amp 0.084251050110757 Neg amp -0.08530413757977995
Chelton Number 170.22168598454567 Chelton Pos amp 5.291564971943509 Chelton Neg
amp -5.128095846325381 ACCESS Number 311.68099516009386 ACCESS Pos amp 0.06803317095123791
ACCESS Neg amp -0.04969146684717923

```

Overall, we observe a polewards decrease in the number of the eddies. This supports the idea that the satellite observations are consistent with a continue dataset.

Global - Climatology - Seasonality

Regions Individual regions

Show positive vs negative amplitudes

4 Trends

5 Summary and Conclusions

Acknowledgments

References

- Chelton, D. B., Schlax, M. G., Samelson, R. M., & de Szoeke, R. A. (2007). Global observations of large oceanic eddies. *Geophysical Research Letters*, 34(15), L15606. doi: 10.1029/2007GL030812
- Martínez-Moreno, J., Hogg, A. M., Kiss, A. E., Constantinou, N. C., & Morison, A. K. (2019). Kinetic energy of eddy-like features from sea surface altimetry. *Journal of Advances in Modeling Earth Systems*, 0(ja). doi: 10.1029/2019MS001769